Polymer 55 (2014) 1061–1069

Contents lists available at ScienceDirect

Polymer

journal homepage: www.elsevier.com/locate/polymer

Dynamic response of transiently trapped entanglements in polymer networks

Diana C. Agudelo [a], Leandro E. Roth [a], Daniel A. Vega [b,*], Enrique M. Vallés [a], Marcelo A. Villar [a]

[a] Department of Chemical Engineering, Planta Piloto de Ingeniería Química, Camino La Carrindanga Km. 7, Universidad Nacional del Sur, CONICET, CC 717, 8000 Bahía Blanca, Argentina
[b] Department of Physics, Instituto de Física del Sur (IFISUR), Universidad Nacional del Sur, CONICET, Av. L.N. Alem 1253, 8000 Bahía Blanca, Argentina

ARTICLE INFO

Article history:
Received 9 November 2013
Received in revised form
31 December 2013
Accepted 8 January 2014
Available online 16 January 2014

Keywords:
Model networks
Pendant chains
Dangling chains

ABSTRACT

The structure and viscoelastic response of polymer networks are highly sensitive to the presence of pendant chains. These imperfections, that are unavoidable produced during a cross-linking reaction, reduce the cross-linking density and affect the damping response of elastomers. In this work the dynamics of pendant chains present in a cross-linked network is investigated using end-linked poly(-dimethyl-siloxane) networks with well defined structure. For this purpose, model networks containing 10 and 20 wt% of two different monodisperse pendant chains with molecular weights well above the critical entanglement molecular weight and some of their blends were prepared. It was found that, within this range of concentration of pendant chains, the long-time dynamic response of the networks was nearly insensitive to the content of pendant material but deeply influenced by the average molar mass of these defects. While the equilibrium behavior of the networks can be well described by a mean field theory for rubber elasticity, the long time relaxational dynamics can be rationalized in terms of the Pearson-Helfand picture for the arm retraction process. Within this theoretical picture, the dynamics can be explained in terms of the molecular architecture of the network, the Rouse time and the weight average molar mass of the pendant material.

1. Introduction

During the last decades linear viscoelastic properties of model polymers melts with complex architectures, like star, combs or hyperbranched molecules have been extensively studied [1–9]. For those systems, it has been found that dynamic properties can be rationalized in terms of a Rouse-like dynamics at short time-scales and the tube model, originally introduced by de Gennes [10] and Doi and Edwards [11], at intermediate and long time-scales. According to this theoretical picture, the slow dynamics of highly entangled melts is strongly dependent on the molecular topology while at short time scales the viscoelasticity is more insensitive to the molecular details [6,11].

Although a similar theoretical picture can be employed to describe the relaxational dynamics of elastomers [12–15], the complexity of the network together with a myriad of structural defects [16,17] significantly increase the diversity of mechanisms involved in the dynamic response.

Most widely used cross-linking techniques, like vulcanization, photo-irradiation or peroxide curing usually lead to a highly complex network structure with a large fraction of defects, like soluble and pendant material which do not contribute to equilibrium properties [18–21]. However, while these defects have a deleterious effect on the equilibrium modulus [22], they usually lead to a slow dynamics that can be advantageous in different applications. One example is on the noise or vibration suppression devices where the damping response is important [23].

In random networks an accurate description of the relationship between molecular structure and viscoelastic properties becomes extremely difficult due uncertainties about molecular features such as molar mass and concentration of pendant and soluble material, molar mass distribution, degree of branching, etc [13].

In opposition to randomly cross-linked systems, model polymer networks obtained via end-linking methods allow a more accurate control of the molecular structure of the network, letting to unveil the role of the different defects on the dynamical response under different external stimuli [17,24–32].

Model polymer networks have been extensively employed to test different theories of rubber elasticity and the contribution of

* Corresponding author.
E-mail address: dvega@criba.edu.ar (D.A. Vega).

0032-3861/$ – see front matter © 2014 Elsevier Ltd. All rights reserved.
http://dx.doi.org/10.1016/j.polymer.2014.01.010

entanglements to the elastic modulus [33–35]. They have also been employed to analyze the effect of soluble and pendant material on the relaxational dynamics. From a microscopic point of view, both elasticity and relaxational dynamics of pendant and elastic material have also been studied through different Nuclear Magnetic Resonance (NMR) techniques [36–40].

In particular, it has been observed that the presence of pendant chains in a network is completely unavoidable in experimental systems [36]. On the other hand, pendant chains, which dominate the slow dynamics, show similar features to those observed in melts of well entangled branched molecules [1,6,11].

In entangled linear polymers, the slow relaxational dynamics is given by the diffusion of molecules along its own contour, a process known as "reptation" [11]. Differently from linear chains, entangled branched molecules cannot reptate to recover equilibrium configurations [1,6,11]. In this case, the reptation is severely suppressed and the chains renew their configurations through a different mechanism, named *arm retraction*, in which the end of each arm independently retracts pathway down its confining tube and then loose the memory of its early configuration reemerging along a different path [1,4,6]. This process is entropically unfavorable and the time scale for complete retraction in the entangled regime increases roughly exponentially with the size of the branch [1,11]. Based on the probability distribution of the primitive path lengths at equilibrium and the tube diameter in melts, the dynamics of a free-end arm can be described as a Brownian motion in a suitable potential field [1]. The potential field for arm retraction comes from the tube model calculation of the plateau modulus of the melt (G_0) and the definition of the molar mass between entanglements, M_e. Pearson-Helfand (PH) model predicts that this potential depends quadratically on the number of entanglements in which the arm is involved. It also postulates that the time required to retract the free end to the branching point grows exponentially with the length of the arm [1]. When compared with experiments employing symmetric star polymer melts, it has been shown that this model over-predicts the terminal relaxation time and the zero-shear viscosity, indicating that the strength of PH arm retraction potential is too high [4,6]. In order to remove this discrepancy, it is necessary to include a dynamic dilution effect that speed up the relaxation dynamics. By including this effect a parameter free model has been developed which accurately describes the viscoelasticity of a wide variety of well entangled branched molecules [4–6].

Since in elastomers the cross-linked lattice provides a roughly fixed network of obstacles for the diffusion of defects, there are no dynamic dilution effects and the original picture of the tube model is recovered. In a network, the constrain release mechanism is severely suppressed [15] and the tube diameter remains roughly constant. Consequently, model networks can be employed to explore the viscoelasticity associated to soluble and pendant material. However, given the slow dynamics associated to pendant chains, its presence largely dominates the terminal relaxation regime. Note that the terminal relaxation time associated to a pendant chain depends exponentially on its molar mass [1]. Thus, it turns out to be extremely large even for moderately entangled chains [15]. Interestingly, since the dynamic dilution is suppressed, the size of the confining tube is fixed and the relaxational dynamics of stars shaped molecules trapped in polymer networks becomes drastically slower than the relaxational dynamics of star melts [15].

Curro and Pincus [12] and Curro et al. [13] developed a model for the relaxation of linear pendant chains in randomly cross-linked polymer networks. The model includes the arm retraction mechanism proposed by Pearson and Helfand [1] and the expected molar mass distribution of pendant material obtained in a random cross-linking reaction. This model successfully predicts the long time behavior of polymer networks and also allows to relate the cross-linking density to the terminal viscoelastic behavior [12,14].

Previously, we have explored the effect of pendant chains on the viscoelastic response of model silicone networks [14,15]. Those model networks were prepared by the reaction between a difunctional poly(dimethylsiloxane) with end vinyl groups (B_2) and a trifunctional silane ended cross-linker (A_3), with a prescribed content of quasi-monodisperse linear molecules of different molar masses with a vinyl group in one end, ω-vinyl poly(-dimethylsiloxane) (B_1). Fig. 1 shows a schematic representation of the network structure obtained through this chemical reaction. Although the final structure of the network is mainly dictated by the relative contents of the precursors, it must be noted that the presence of undesired defects is unavoidable. Steric effects and the presence of non-reactive polymer precursor limit the maximum extent of reaction and the content of soluble material in the network cannot be reduced below ~2 wt%. Consequently, the viscoelasticity of the networks is affected by these defects that reduce the equilibrium elastic modulus and increase the dissipation at long times (Fig. 1).

For these systems the relaxation modulus shows, at long times, a similar behavior to that observed in random networks, where the relaxation modulus can be well described by the empirical equation proposed by Chasset–Thirion [41–43]

$$G(t) = G_\infty \left[1 + \left(\frac{\tau_C}{t}\right)^m\right] \quad (1)$$

where $G(t)$ is the relaxation modulus at the reference temperature T_0, G_∞ is the equilibrium modulus, and m and τ_C are characteristic parameters stated by the network structure and microscopic timescales [12–14].

Previously, we extended the model proposed by Curro and Pincus by including an arbitrary distribution of molar masses of pendant chains [14]. With this modification, the model successfully predicts the long time relaxation process of networks obtained with an approximately constant degree of cross-linking and pendant chains of different molar masses. In addition, it was shown that the Chasset–Thirion exponent m is a function of molar mass and polydispersity of the pendant chains [14]. A more refined

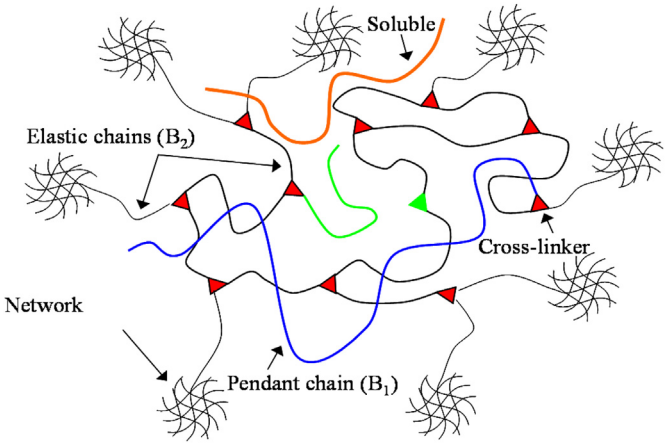

Fig. 1. Schematic representation of polymer networks employed in this study. Note that linear pendant chains (B_1) are linked to the network structure only through one of the chain ends. The presence of soluble material (orange line) is always unavoidable. Partially unreacted cross-linkers (green triangle) and difunctional chains B_2 (green line) also lead to a reduction in the elasticity and the appearance of slow relaxing defects. (For interpretation of the references to color in this figure legend, the reader is referred to the web version of this article.)

parameters-free model was also employed to describe the relaxation modulus of model silicone networks [15]. In this case, it was found that dynamic dilution must not be considered in order to describe the arm retraction in networks, in agreement with the theoretical prediction of de Gennes for the dynamics of dangling ends diffusing in a fixed network of obstacles [10].

Model networks were also employed to analyze the effect of the concentration of pendant material on the terminal relaxation dynamics. In this case, it was found that the slow dynamics is relatively insensitive to the content of pendant material, while equilibrium properties were more strongly affected [22].

In this paper we analyze the effect of the molar mass distribution of pendant chains on the equilibrium and dynamical properties of polymer networks. We studied model networks prepared with linear bimodal pendant chains, with two fixed concentrations of this type of defects (10 and 20 wt%). The bimodality of pendant chains was obtained through the mixture of two monofunctional polymers with different molar mass distribution and the subsequent reaction with the network precursors. Equilibrium and non-equilibrium properties are rationalized in terms of a mean field model that describes the network structure [15] and a model based on the arm retraction process in a Pearson-Helfand potential [1].

2. Experimental

Model poly(dimethylsiloxane) networks were obtained by a hydrosilylation reaction, based on the addition of hydrogen silanes from cross-linker molecules to end vinyl groups present in prepolymer molecules [44]. A commercial difunctional prepolymer, α,ω-divinyl poly(dimethylsiloxane) (B_2) (United Chemical Technology, Inc.) and mixtures of two monodisperse monofunctional prepolymers, ω-vinyl poly(dimethylsiloxane) ($B_{1,1}$ and $B_{1,2}$) with different molar masses were employed. The molar mass characterization of the prepolymers and other reactants used in the cross-linking reactions are listed in Table 1 where the notation $B_{1,i}$, with $i = 1, 2$, was employed for the monofunctional ω-vinyl poly(-dimethylsiloxane) chains. Phenyltris(dimethylsiloxy)silane (A_3) (United Chemical Technology, Inc.) was used as cross-linker and a Pt salt was employed as catalyst for the cross-linking reaction. Monofunctional prepolymers ($B_{1,i}$) were synthesized by anionic polymerization using n-butyllithium as initiator, n-hexane as solvent and THF as polymerization promoter, which allowed us to obtain polymers with a narrow molar mass distribution [30].

Mixtures of monofunctional prepolymers ($B_{1,i}$) were prepared in order to obtain model networks containing linear bimodal pendant chains. These mixtures were prepared at different relative percentages of each of the monofunctional prepolymers and their average molar masses were calculated with the following expressions [45]:

$$M_{n_B} = \frac{1}{\sum_{i=1}^{n}\left(W_{B_{1,i}}/M_{n_{B_{1,i}}}\right)} = \sum_{i=1}^{n}\left(N_{B_{1,i}}M_{n_{B_{1,i}}}\right) \quad (2)$$

$$M_{w_B} = \sum_{i=1}^{n}\left(W_{B_{1,i}}M_{w_{B_{1,i}}}\right) \quad (3)$$

where $W_{B_{1,i}}$ and $N_{B_{1,i}}$ are the mass and number fraction of monofunctional polymers with number ($M_{n_{B_{1,i}}}$) and weight ($M_{w_{B_{1,i}}}$) average molar mass respectively. The subscript "B" denotes the binary mixture [45].

The composition of the different binary blends employed in the synthesis of model networks containing linear bimodal pendant chains is shown in Table 2.

To prepare the networks, the blend of the monofunctional monodisperse polymers was mechanically stirred for 2 h. The prepolymers and the cross-linker were weighted in order to obtain stoichiometrically balanced mixtures with two concentrations (10 and 20 wt%) of the different blends of monofunctional polymers. Reactants were mixed with a mechanical stirrer and degassed under vacuum to eliminate bubbles. The reactive mixture was then placed between the plates of a mechanical spectrometer (Rheometrics Dynamic Analyzer RDA-II). Cure reactions were carried out at 333 K and final properties were measured after 24 h of reaction. Dynamic and stress relaxation measurements were done, under nitrogen atmosphere, in the temperature range of 243–473 K using 25-mm parallel plates. Elastic modulus, $G'(\omega)$, and loss modulus, $G''(\omega)$, in the range of 0.05–500 rad/s and relaxation modulus, $G(t)$, as function of time were obtained with deformations of up to 20% within the range of linear viscoelastic response.

After viscoelastic measurements, networks were subjected to soluble extraction using toluene as solvent. Samples were weighed and placed in glass jars with solvent to remove the non-cross-linked polymer. Soluble extraction was carried out at room temperature for about one month, and solvent was replaced every 3–4 days. Following extraction, samples were weighed and dried under vacuum at 313 K until complete solvent removal was achieved. Dry networks were weighed again, and the weight fraction of soluble (W_S) and the volume fraction of polymer in the equilibrium swollen network (ν_{2m}) were calculated (see also Ref. [46]).

3. Results and discussion

3.1. Molecular structure

Molecular structure of a polymeric network is strongly influenced by the final extent of reaction reached during the cross-linking process. As mentioned above, at complete reaction even stoichiometrically balanced networks contain defects. Consequently, in any real system the presence of solubles is completely unavoidable [46]. Previously, it has been found that ideal conditions (lowest soluble content) can be approached when a slight excess of cross-linker is incorporated in the formulation. Previous work with similar networks prepared without pendant chains, i.e. cross-linking the α,ω-divinyl poly(dimethylsiloxanes) with a trifunctional cross-linker (A_3 + B_2), allowed to establish that a minimum soluble fraction (W_S) of about 3% was obtained when a stoichiometric imbalance $r = 1.15$ was employed [47]. Under these

Table 1
Molecular characterization of linear prepolymers and other reactants used for the preparation of model PDMS networks.

Polymer	M_n FTIR (g/mol)	M_n SEC (g/mol)	M_w SEC (g/mol)	M_w/M_n SEC
B_2	7200	7300	21,500	2.95
$B_{1,1}$	46,300	47,800	51,300	1.07
$B_{1,2}$	96,600	97,200	121,300	1.14

Cross-linker $(HSi(CH_3)_2O)_3SiC_6H_5$ (A_3).
Catalyst *cis*-$Pt((C_2H_5)_2S)_2Cl_2$.

Table 2
Characterization of the binary mixtures of monofunctional monodisperse polymers ($B_{1,1}$ and $B_{1,2}$).

Mixture	$W_{B_{1,1}}$ (g/g)	$N_{B_{1,1}}$ (mol/mol)	M_{n_m} (g/mol)	M_{w_m} (g/mol)	M_w/M_n
A	0.000	0.000	97,200	121,000	1.25
B	0.252	0.406	77,100	104,000	1.35
C	0.503	0.673	64,000	86,100	1.35
D	0.737	0.851	55,200	69,700	1.26
E	1.000	1.000	47,800	51,300	1.07

conditions, it was found that the content of elastically active chains, and thus the equilibrium modulus (G_∞), and the volume fraction of polymer in the equilibrium swollen network (ν_{2m}) are maximized [47].

Table 3 shows the nomenclature, composition and some relevant characteristics of the model networks studied. In this table the second and third columns contain information related to networks composition, such as the total weight fraction of monofunctional polymers in the model networks (W_m) and the stoichiometric imbalance (r). Taking the values of W_S and r at the optimum experimental conditions, we have referred the reported stoichiometric imbalances and soluble fractions to those corresponding to the optimum values, i.e. the reported stoichiometric imbalances and soluble fractions are calculated as $r = r_{exp}/1.15$ and $W_S = W_{S_{exp}} - 0.03$, where the sub index 'exp' indicates the actual values of imbalance employed in the reaction and the soluble fraction measured in the different networks (see also Ref. [22]). Column fourth to seventh correspond to experimental values of the volume fraction of polymer in the equilibrium swollen network (ν_{2m}), the weight fraction of solubles (W_S), the maximum extent of reaction (p_∞), calculated from W_S using the recursive method described elsewhere [48–51] and the elastic modulus measured in the limit of low frequencies ($G'_{\omega\to 0}$) at a reference temperature of 273 K. The last column shows the theoretically predicted values of shear equilibrium modulus calculated from the experimental values using the recursive method [48–51]. In the recursive model the reactive system $A_3 + B_2 + B_{1,1} + B_{1,2}$ was considered as a terpolymerization $A_3 + B_2 + B_1$, where B_1 represents the binary mixture of monofunctional polymers.

Equilibrium properties show a significant variation when the content of linear bimodal pendant chains increases from 10 to 20 wt% in the network (Table 3). The increment in the concentration of pendant chains induces a reduction in the density of elastically active chains (ν), and consequently a reduction in ν_{2m} and $G'_{\omega\to 0}$, in agreement with classical theories for rubber elasticity [22].

On the other hand, at a given concentration of linear bimodal pendant chains (10 or 20 wt%) experimental values show a slight increase in the fraction of soluble material and a reduction in elasticity as dangling material becomes richer in polymer $B_{1,1}$. This behavior is also in agreement with the theory. At a fixed weight content of pendant chains, a reduction in the average molar mass of dangling chains increases the content of elastically active cross-linker nodes that are removed (each dangling chain B_1 "disable" one reactive group of the cross-linker agent).

As the maximum extent of reaction is within the range $p_\infty \sim 0.93$–0.94 (Table 3) network contains unreacted or partially reacted B_1 and B_2 chains. Note that while completely unreacted B_1 and B_2 chains contribute to the soluble material; partially reacted B_2 chains become pendant chains. In our case, the content of pendant material coming from B_2 can be estimated through the recursive model and it is between 8 and 10 wt% [38]. The same model can also be employed to determine the content of reacted B_1 chains. In this case, it can be shown that more than 93% of the monofunctional polymer incorporated to the reactive mixture has reacted. Is important to take into account that although an important content of difunctional polymer acting as pendant material is present, this will not influence the behavior of the viscoelastic properties measured at low frequencies or long times. Given the strong dependence of relaxation times of pendant chains with the molar mass (see below), the relaxational spectrum corresponding to each species (B_1 and B_2) is quite different.

While for the difunctional polymer used here the average molar mass is close to the molar mass between entanglements ($M_e \sim 9800$ g/mol [52]), monofunctional chains are well entangled and thus have a much slower dynamics. In the next sections we analyze the dynamic response of polymer networks described in Table 3.

Table 3
Nomenclature and main characteristics of model networks prepared.

Network	W_m (g/g)	r	ν_{2m} (V/V)	W_S (g/g)	p_∞	$G'_{\omega\to 0}$ (MPa)	
						Exptl.	Eq. (5)[a]
B_2-A-10	0.097	1.007	0.241	0.010	0.943	0.215	0.208
B_2-B-10	0.099	1.006	0.239	0.011	0.942	0.211	0.205
B_2-C-10	0.097	1.002	0.238	0.011	0.944	0.206	0.204
B_2-D-10	0.098	1.013	0.238	0.012	0.935	0.203	0.201
B_2-E-10	0.097	1.012	0.235	0.012	0.934	0.201	0.198
B_2-A-20	0.195	1.007	0.225	0.022	0.932	0.180	0.184
B_2-B-20	0.198	1.006	0.224	0.023	0.931	0.178	0.181
B_2-C-20	0.196	0.997	0.222	0.024	0.936	0.176	0.178
B_2-D-20	0.195	1.003	0.222	0.024	0.932	0.173	0.177
B_2-E-20	0.195	1.008	0.221	0.025	0.928	0.168	0.176

[a] Values of $h = 1$ and $G_e = 0.8\, G_N^0$ were used in all calculations, assuming 0.195 MPa as plateau modulus of PDMS at 273 K [44].

3.2. Elastic response and equilibrium properties

Fig. 2 shows master curves of elastic modulus (G') as a function of frequency (ω) for networks prepared with 10 wt% and 20 wt% of monofunctional chains, at a reference temperature of 273 K. G'

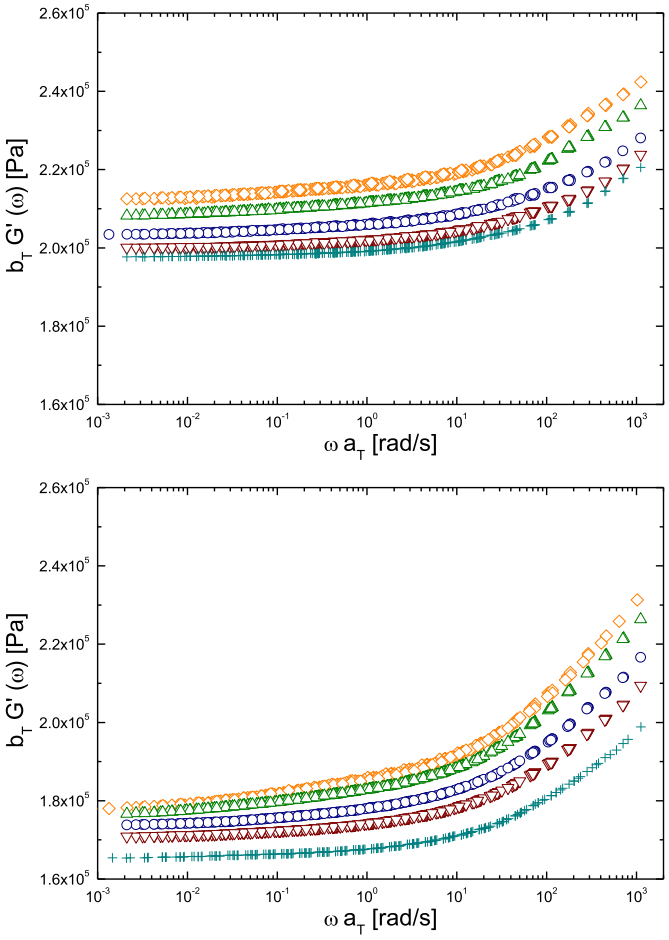

Fig. 2. Master curves of storage modulus (G') as a function of frequency (ω). $T_0 = 273$ K. Networks prepared with 10 wt% (top) and 20 wt% (bottom) of monofunctional chains. Symbols: (+) 100 wt% of $B_{1,1}$, (▽) ~75 wt% of $B_{1,1}$, (○) ~50 wt% of $B_{1,1}$, (△) ~25 wt% of $B_{1,1}$, (◇) 0 wt% of $B_{1,1}$.

decreases as the content of linear pendants $B_{1,1}$ increases. This result can be rationalized in terms of the density of elastically active chains. As it was pointed out above, at a fixed weight content of pendant chains, as the average molar mass of the dangling chains decreases (amount of $B_{1,1}$ chains increases) the content of elastically active cross-linker nodes decreases. This dependence is emphasized in Fig. 3 that shows the behavior of the shear elastic modulus in the limit of low frequencies ($G'_{\omega\to 0}$) as a function of the weight percent of $B_{1,1}$. As expected, shear equilibrium modulus decreases gradually as the concentration of $B_{1,1}$ in the pendant material increases. Also, equilibrium modulus decreases when the global concentration of bimodal linear pendant chains in the networks increases from 10 to 20 wt%. In this case, the strong dependence of the elastic response with the content of pendant chains is in good agreement with previous experiments with a similar system [22] and can be attributed to the strong reduction in the concentration of elastically active chains. The inset of Fig. 3 also shows ν_{2m} as a function of the content of $B_{1,1}$. As ν_{2m} is also a measure of the elasticity of the networks, its behavior shows similar features to those observed in $G'_{\omega\to 0}$.

On the other hand, experimental results shown in Fig. 2 demonstrate that elastic modulus is a monotonously growing function of the frequency. According to the arm retraction model, the time required to retract the free end of a pendant chain to the cross-linking point depends exponentially with the length of the arm and implies a very broad spectrum of relaxation times. Thus, while at very low frequencies pendant chains are partially relaxed (dynamically disentangled) and cannot contribute to the transient elastic response, as the frequency increases an increasing fraction of the pendant chains becomes involved in the elastic response. That is, as the frequency increases a larger fraction on the pendant chains act as being entangled.

Theoretical predictions for the elastic modulus in terms of network parameters can be obtained through different models. Particularly, those models that incorporate both network equilibrium structure and trapped entanglements have been widely employed to describe swelling and equilibrium properties [53]. One of the simplest models that describe network elasticity considering the contribution of trapped entanglements was proposed by Langley and Polmanteer [33]:

$$G'_{\omega\to 0} = (\nu - h\mu)\mathrm{RT} + G_e T_e \quad (4)$$

here ν is the concentration of elastically active chains, h an empirical constant (taking values between 0 and 1), μ the concentration of cross-linking points, R the gas constant, and T the absolute temperature. T_e is the fraction of trapped entanglements and G_e is the contribution to the modulus by the trapped entanglements. Experimental and theoretical calculations indicate that G_e is approximately 0.8 G_N^0, where G_N^0 is the plateau modulus of the molten polymer [11]. Table 3 shows the values predicted by the recursive model [48–51] and the experimental data. Note that predictions of this model agree within the 5% with the experimental values obtained through rheology.

3.3. Loss modulus $G''(\omega)$

Fig. 4 shows master curves of loss modulus (G'') as a function of frequency (ω) for the networks prepared with 10 wt% and with 20 wt% of monofunctional chains. For both concentrations, the loss modulus increases with the content of monofunctional polymer $B_{1,2}$ in the network. However, note that in the high frequency regime G'' becomes more insensitive to the network structure. In this zone the relaxation spectrum of the network is governed by the segmental motions of the different chains and the dissipative

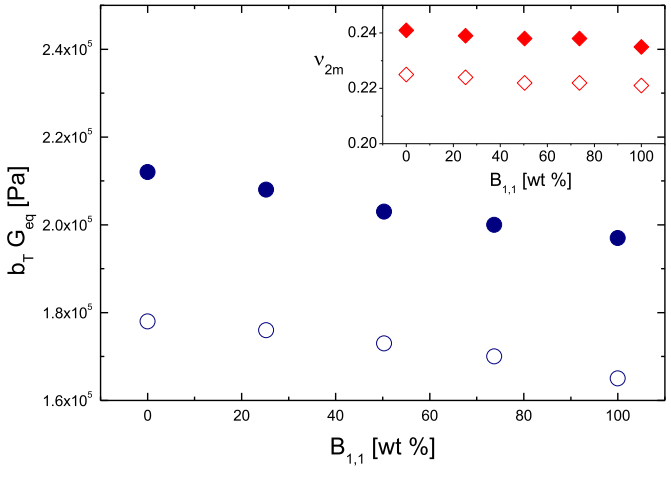

Fig. 3. Elastic modulus in equilibrium ($G_{eq} = G'_{\omega\to 0}$) as a function of weight percentage of $B_{1,1}$ (wt%) in the binary mixture of monofunctional polymers, $T_0 = 273$ K. Symbols: (●) Networks with 10 wt% of monofunctional polymer chains, and (○) networks with 20 wt% of monofunctional polymer chains. Inset: ν_{2m} as a function of weight percentage of $B_{1,1}$. Filled symbols: Networks with 10 wt% of monofunctional polymer chains. Open symbols: networks with 20 wt% of monofunctional polymer chains.

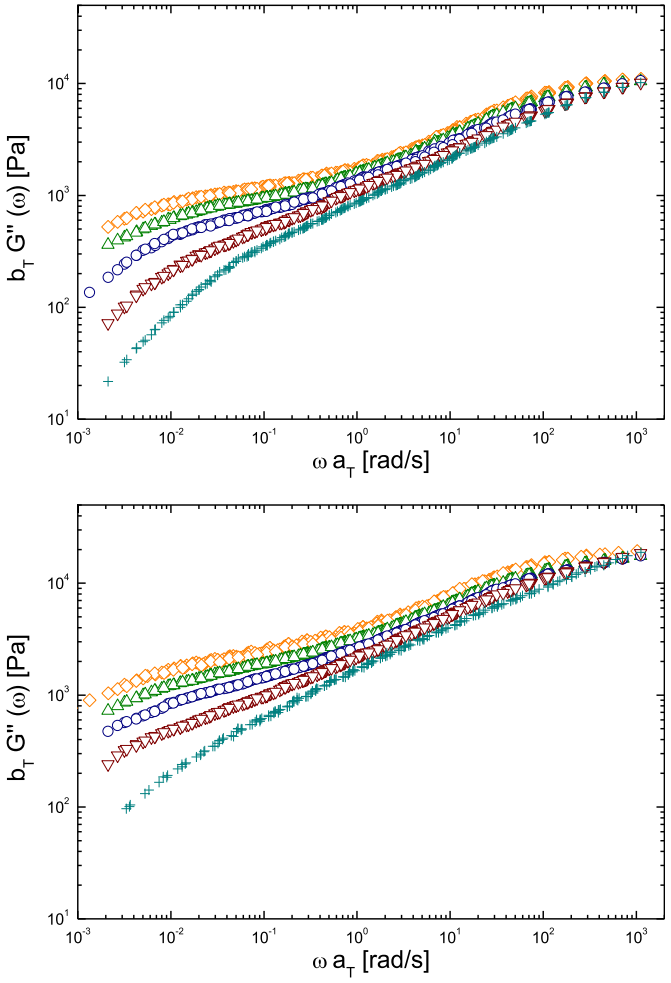

Fig. 4. Master curves of loss modulus (G'') as a function of frequency (ω). $T_0 = 273$ K. Networks prepared with 10 wt% (top) and 20 wt% (bottom) of monofunctional chains. Symbols: (+) 100 wt% of $B_{1,1}$, (▽) ~75 wt% of $B_{1,1}$, (○) ~50 wt% of $B_{1,1}$, (△) ~25 wt% of $B_{1,1}$, (◇) 0 wt% of $B_{1,1}$.

dynamics becomes independent on the details of the molecular structure of the defects.

In contrast, at low frequencies the effect of the molar mass of pendant material is clearly unveiled. Note that even though in the frequency range explored here the different systems do not reach the terminal regime, where $G'' \sim \omega^{-1}$, the difference among the networks studied is notorious. In Fig. 3 can also be observed a tendency to form a slight plateau in G'' at frequencies around 10^{-1} rad/s. This plateau is a clear indication of the presence of transiently trapped entanglements that also contribute to G' in this frequency regime. Taking into account that molar mass of $B_{1,2}$ chains is about twice the corresponding to $B_{1,1}$ chains, the width of the plateau increases while the terminal regime shift towards lower frequencies as the content of the longest B_1 chains increases.

In order to test these results against the arm retraction process that leads the dynamics of pendant chains in the long time regime, terminal relaxation times can be estimated through the Pearson-Helfand model for chains with an end attached to a cross-linking point and the other moving under the action of the PH potential [1], that reads as: $U_{PH} = (15/8)n_e^2 s$, where s $(0 < s < 1)$ is the fractional distance back along the primitive path where the free end has been retracted. According to this model, the relaxation time can be expressed as [15]:

$$\tau(s, n_e) = -\frac{15}{16}\frac{I\pi^3 n_e^2 \tau_e}{\alpha}\,\mathrm{erf}(I\sqrt{\alpha n_e}s) \tag{5}$$

where n_e is the average number of segments per entanglement, τ_e is the Rouse relaxation time for a chain of length n_e, $\alpha = 7/3$, $I = \sqrt{-1}$ and erf $[x]$ is the error function [15].

Taking into account the number average molar mass of pendant chains and the Rouse time and average molar mass between entanglements [15,52], τ_e and M_e, respectively, it is possible to obtain the largest longitudinal Rouse time and an upper bound for the terminal relaxation time of the pendant chains (note that transverse Rouse modes on time scales longer than τ_e are forbidden by the confining tube [4,11]). For a fully retracted pendant chain we have $\tau \sim 2$ s for $B_{1,1}$ chains and $\tau \sim 5\,10^3$ s for $B_{1,2}$ chains. Note that while pendant chains are relatively monodisperse and these time-scales are estimated here through the number average molar mass M_n of the chains, their molar mass distribution follows a log-normal distribution [14], that implies small contents of relatively high molar mass chains and thus, larger time scales for complete retraction must be expected. The same calculation employing the Milner-McLeish potential ($U_{MM} = (27/56)n_e^2$ for a fully retracted chain) [4], that agrees quite well with the experimental data of entangled star polymer melts leads to $\tau \sim 0.01$ s for $B_{1,1}$ chains and $\tau \sim 0.2$ s for $B_{1,2}$ chains.

On the other hand, the largest Rouse time for the pendant chains can be estimated as follows [4]. According to the tube model, at short time scales relaxation of pendant chains is dictated by a Rouse like dynamics. At these time scales the arm retraction potential is small and can be neglected. Within this approach, the largest Rouse time for the "free diffusion" of pendant chains can be expressed as $\tau_R(s, n_e) \sim (225/256)\pi^3 n_e^2$, that for $B_{1,1}$ chains corresponds to $\tau_R \sim 1 \times 10^{-3}$ s while for $B_{1,2}$ chains is $\tau_R \sim 4 \times 10^{-3}$ s, both well below the terminal regime.

Therefore, we can conclude that a Pearson-Helfand potential is in rough agreement with the experiments indicating that neither $B_{1,1}$ nor $B_{1,2}$ chains reaches equilibrium in the frequency scales explored here.

As pointed out above, for a given molar mass distribution of pendant material, equilibrium properties are deeply affected by the concentration of pendant chains due to their deleterious effect on the concentration of elastically active chains. However, while this effect reduces the network elasticity and increases the dissipation, in the low concentration regime (without self-entanglements) the content of pendant chains does not affect the relaxation spectrum.

Fig. 5 compares the loss and elastic modulus for networks containing different contents of pendant chains of fixed average molar mass. Note that upon vertical rescaling of G' and G'' the curves corresponding to both concentrations overlap quite nicely, clearly indicating that the width of the relaxation spectrum remains essentially unaffected by the concentration of pendant

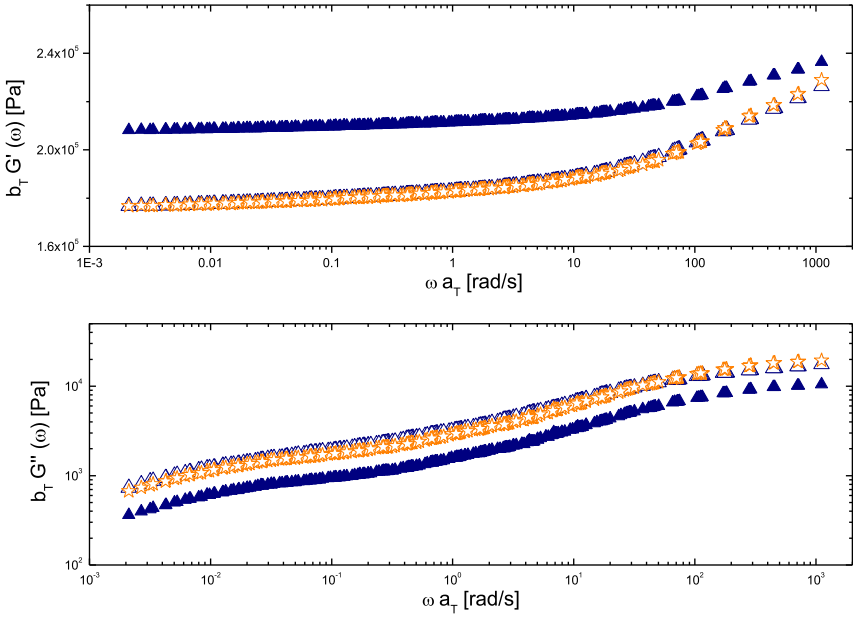

Fig. 5. Master curves of storage (top) and loss modulus (bottom) as a function of frequency (ω) at $T_0 = 273$ K for networks prepared with 10 wt% (▲) and 20 wt% (△) of pendant chains (75 wt% of $B_{1,1}$). Filled symbols represents the data of networks containing 20 wt% of pendant chains rescaled and vertically shifted to compare with the data corresponding to networks with 10 wt% of pendant chains. In order to overlap the curves, data corresponding to $G''(\omega)$ and $G'(\omega)$ where multiplied by a factor of 1.85. In addition, $G'(\omega)$ was also vertically shifted by a factor of 0.208 MPa.

chains. As here there are no dilution dynamic effects and the self entanglement probability among pendant chains is quite low, even for the samples with the highest content of defects, the relaxation spectrum is insensitive to the concentration of the pendant chains. This result agrees with the theory that predicts that in the low concentration regime the relaxation spectrum is independent of the content of pendant chains [14,15].

3.4. Relaxation modulus, G(t)

While the dynamic moduli $G^*(\omega)$ provides relevant information about the relaxational dynamics of polymer networks, stress relaxation experiments are more appropriated to test the long time regime.

Fig. 6 shows master curves of relaxation modulus $G(t)$ as a function of time (t) at reference temperature of 273 K for networks prepared with 10 wt% and 20 wt% of monofunctional chains.

In agreement with previous results for the dynamic moduli, the long time relaxation modulus decreases with the concentration of elastically active chains (ν), that is affected by the concentration and average molar mass of the pendant material. On the other hand, as expected, network relaxation is slower when the content of dangling $B_{1,2}$ chains increases.

Several models have been proposed in order to describe the relaxational response of elastomers [41–43]. Independently of the specific technique of synthesis, it has been found that the power law dependence on time of the relaxation modulus (Eqn. (1)) comes from the slow relaxation of pendant material.

In networks obtained by random cross-linking techniques, the exponent "m" in the Chasset–Thirion equation is dictated by the degree of cross-linking, that controls the average molar mass of the pendant chains [13]. In this case, the typical values of m are located in the range of ~0.1–0.3. On the other hand, in model networks obtained by end-linking techniques it has been found that the exponent can increase up to $m \sim 1$ for systems containing low molar mass pendant chains [14].

Fig. 6 also shows the fit of $G(t)$ with the Thirion–Chasset equation in the long time regime. In agreement with previous results, here we observe that this equation describes adequately $G(t)$ over several decades. Figs. 7 and 8 show the behavior of the Chasset–Thirion parameters, the exponent m and the characteristic time τ_C, for two different concentrations of pendant material as a function of weight percentage of $B_{1,1}$. Note that while m is nearly independent of the concentration, it slightly increases as the average molar mass of the pendant chains decreases, the characteristic time τ_C changes over several orders of magnitude as a function of weight percentage of $B_{1,1}$ and it is also dependent of the total content of pendant material.

Based on the arm retraction mechanism, it has been proposed that the exponent m is mainly affected by the weight average molar mass of pendant chains [14]:

$$m = a\left(M_{w_p}\right)^{-b} \tag{6}$$

where a and b are constants, and M_w represents the weight average molar mass of pendant chains. On the other hand, theory predicts that constant b is close to unit [14]. The inset of Fig. 7 shows m as a function of M_w for networks prepared with 10 wt% and 20 wt% of pendant chains. Note that m follows a power law with M_w with an exponent very close to the one predicted by the theory ($m \sim M_w^{-1.3}$).

Although the characteristic time τ_C depends strongly on the networks architecture, it can be associated to a microscopic time scale. Previously, it was shown that the effect of pendant chains concentration can be included by considering the approximate relationship [22]:

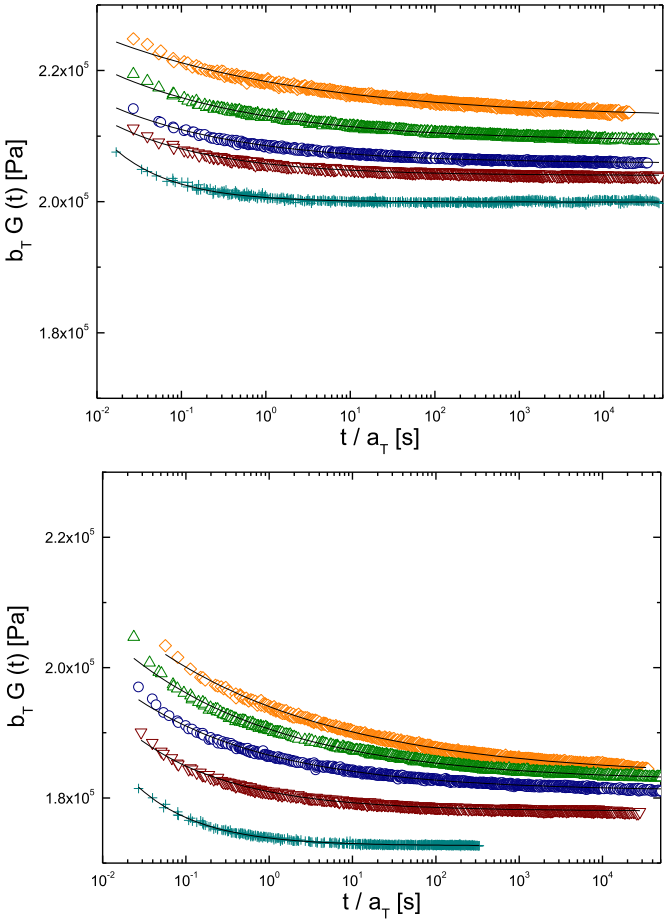

Fig. 6. Master curves of relaxation modulus $G(t)$ as a function of time (t). $T_0 = 273$ K. Top: Networks prepared with 10 wt% of monofunctional chains. Bottom: networks prepared with 20 wt% of monofunctional chains. Symbols: (+) 100 wt% of $B_{1,1}$, (▽) ~75 wt% of $B_{1,1}$, (O) ~50 wt% of $B_{1,1}$, (△) ~25 wt% of $B_{1,1}$, (◇) 0 wt% of $B_{1,1}$. Lines represent the fits with the Thirion–Chasset equation.

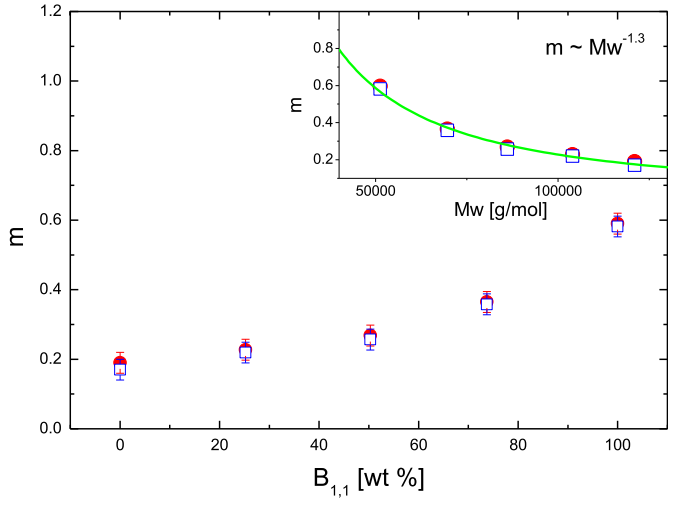

Fig. 7. Parameter "m" of the Chasset–Thirion equation as a function of the weight percentage of $B_{1,1}$ in the binary mixture of monofunctional polymers. Symbols: (●) Networks with 10 wt% of linear bimodal pendant chains, and (□) networks with 20 wt % of linear bimodal pendant chains. Inset: symbols show m as function of the average molar mass (M_w) of the monofunctional chains and the line is a power law fit to the data.

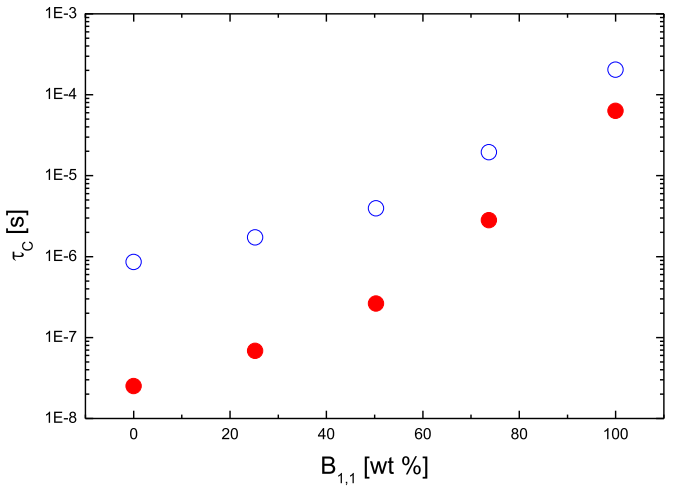

Fig. 8. Parameter "τ_C" of the Chasset–Thirion equation as a function of the weight percentage of $B_{1,1}$ in the binary mixture of monofunctional polymers. Symbols: (●) Networks with 10 wt% of linear bimodal pendant chains, and (○) networks with 20 wt % of linear bimodal pendant chains.

$$G(t) \sim G_\infty \left[1 + \phi \left(\frac{\hat{\tau}_C}{t}\right)^m\right] \tag{7}$$

where ϕ is the concentration of pendant chains and $\hat{\tau}_C = \tau_C \phi^{-1/m}$. Thus, as shown in Fig. 9 the strong dependence of τ_C with pendant chains concentration observed in Fig. 7 can be compensated by the effect of concentration, that scales as $\phi^{-1/m}$. Then, the new characteristic time $\hat{\tau}_C$ becomes roughly independent of concentration. Fig. 9 shows $\tau_C \phi^{-1/m}$ as a function of M_w for both concentrations. We observed that this time scale is closely related to the Rouse time. According to the arm retraction process in a PH potential, at short time scales the free end of pendant chains relax a relatively small distance towards the cross-linking point. Then, the arm retraction potential is irrelevant and pendant free ends relax freely up to time scales where it "discovers" the confining tube at $s = s^* \sim 1/\sqrt{n_e}$ (Eqn. (5)). This time scale, given by $\tau_R(s = s^*) \sim (225/256)\pi^3 n_e^2$ is also plotted in Fig. 9. Note that this simple approach for the dependence of the characteristic time scale

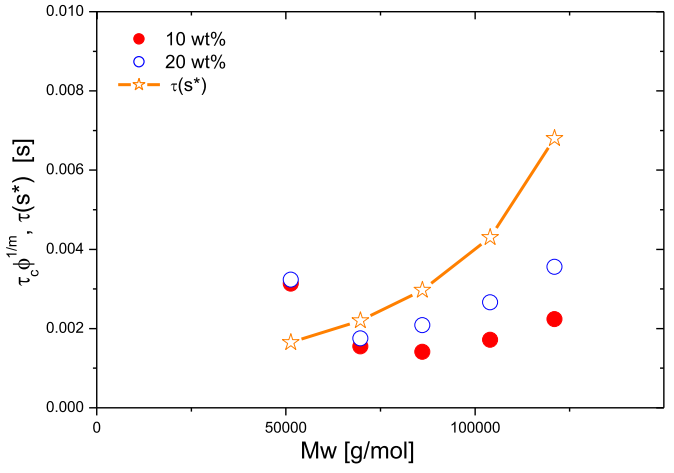

Fig. 9. Parameter "τ_C" of the Chasset–Thirion equation rescaled with the concentration ϕ of pendant chains as a function of weight average molar mass (M_w) of the pendant material. Symbols: (●) Networks with 10 wt% of linear bimodal pendant chains, and (○) networks with 20 wt% of linear bimodal pendant chains. Star symbols correspond to the Rouse time of pendant chains $\tau(s^*)$ (connecting lines are a guide to the eye).

in the Thirion–Chasset model provides a reasonably good description for the experimental data.

4. Conclusions

The end-linking technique allows an accurate control over the equilibrium structure of polymer networks. In agreement with previous experiments in the literature [15,37], we observe that network structure can be nicely described through a classical mean field model. In addition, within the low concentration regime studied here, where there are no self-entanglements among defects, equilibrium properties depends on the concentration of defects, while the relaxation spectrum is strongly affected by the average molar mass of the pendant material.

Polymer networks unavoidably contain defects that dictate their long time dynamics. Among the wide variety of structural defects in a network, high molar mass pendant chains control the terminal relaxation dynamics. For pendant chains, similarly to entangled star polymer melts, the reptation process is inhibited and the relaxational dynamics becomes driven by the arm retraction potential. However, since dynamic dilution effect, that reduces the strength of the arm retraction potential in star melts, is absent; in polymer networks the dynamics becomes drastically slower. Thus, the stress relaxation process occurs under the action of the strong arm retraction potential derived by Pearson and Helfand.

In agreement with previous experiments we have observed that long time relaxation modulus can be described by the Thirion–Chasset equation and the constants in this empirical equation can be related to a parameters free theory that only requires knowing the number of entanglements per pendant chain, its concentration, and the Rouse time among entanglements.

Acknowledgments

We express our gratitude to the Universidad Nacional del Sur (UNS) and the National Research Council of Argentina (CONICET) which supported this work.

References

[1] Pearson DS, Helfand E. Macromolecules 1984;17:888–95.
[2] Bartels CR, Crist B, Fetters LJ, Graessley WW. Macromolecules 1986;19:785–93.
[3] Ball RC, McLeish TCB. Macromolecules 1989;22:1911–3.
[4] Milner ST, McLeish TCB. Macromolecules 1997;30:2159–66.
[5] Frischknecht AL, Milner ST, Pryke A, Young RN, Hawkins R, McLeish TCB. Macromolecules 2002;35:4801–20.
[6] McLeish TCB. Adv Phys 2002;51:1379–527.
[7] Lohse DJ, Milner ST, Fetteres LJ, Xenidou M, Hadjichristidis N, Mendelson RA, et al. Macromolecules 2002;35:3066–75.
[8] Vega DA, Sebastian JM, Russel WB, Register RA. Macromolecules 2002;35:169–77.
[9] Miros A, Vlassopoulos D, Likhtman AE, Roovers J. J Rheol 2003;47:163.
[10] de Gennes. Scaling concepts in polymer physics. Ithaca, New York: Cornell University Press; 1979.
[11] Doi M, Edwards SF. The theory of polymer dynamics. Oxford: Clarendon Press; 1986.
[12] Curro JG, Pincus P. Macromolecules 1983;16:559–62.
[13] Curro JG, Pearson DS, Helfand E. Macromolecules 1985;18:1157–62.
[14] Vega DA, Villar MA, Alessandrini JL, Valles EM. Macromolecules 2001;34:4591–6.
[15] Vega DA, Gómez LR, Roth LE, Ressia JA, Villar MA, Valles EM. Phys Rev Lett 2005;95:166002.
[16] Vallés EM, Macosko CW. Rubber Chem Technol 1976;49:1232–7.
[17] Yamazaki H, Takeda M, Kohno UY, Ando H, Urayama K, Takigawa T. Macromolecules 2011;44:8829–34.
[18] Dickie RA, Ferry JD. J Phys Chem 1966;70:2594–600.
[19] Stepto R. Polymer networks: principles of their formation, structure and properties. 1st ed. London: Chapman and Hall; 1997. pp. 243–87.
[20] Martin G, Barres C, Cassagnau P, Sonntag P, Garois N. Polymer 2008;49:1892–901.
[21] Zhang X, Yang H, Song Y, Zheng Q. Polymer 2012;53:3035–42.

[22] Roth LE, Vega DA, Vallés EM, Villar MA. Polymer 2004;45:5923–31.
[23] Urayama K. Polym J 2008;40:669–78.
[24] Batra A, Cohen C, Archer L. Macromolecules 2005;38:7174–80.
[25] Urayama K, Kawamura T, Kohjiya S. Polymer 2009;50:347–56.
[26] Genesky GD, Cohen C. Polymer 2010;51:4152–9.
[27] Yoo SH, Yee L, Cohen C. Polymer 2010;51:1608–13.
[28] Bibbó MA, Vallés EM. Macromolecules 1984;17:360–5.
[29] Vallés EM, Rost EJ, Macosko CW. Rubber Chem Technol 1984;57:55–62.
[30] Villar MA, Bibbó MA, Vallés EM. J Macromol Sci Part A: Pure Appl Chem 1992;A29(4 & 5):391–400.
[31] Kawamura T, Urayama K, Kohjiya S. Macromolecules 2001;34:8252–60.
[32] Urayama K, Yokoyama K, Kohjiya S. Macromolecules 2001;34:8261–9.
[33] Langley N, Polmanteer K. J Polym Sci Part B: Polym Phys 1974;12:1023–34.
[34] Dossin LM, Graessley WW. Macromolecules 1979;12:123–30.
[35] Pearson DS, Graessley WW. Macromolecules 1980;13:1001–9.
[36] Vega DA, Villar MA, Vallés EM, Steren CA, Monti GA. Macromolecules 2001;34:283–8.
[37] Acosta RH, Vega DA, Villar MA, Monti GA, Valles EM. Macromolecules 2006;39:4788–92.
[38] Acosta RH, Monti GA, Villar MA, Valles EM, Vega DA. Macromolecules 2009;42:4674–80.
[39] Valentín JL, Posadas P, Fernández-Torres A, Malmierca MA, González L, Chassé W, et al. Macromolecules 2010;43:4210–22.
[40] Chassé W, Lang M, Sommer J-U, Saalwächter K. Macromolecules 2012;45:899–912.
[41] Chasset R, Thirion P. In: Prins JA, editor. Proceedings of the conference on physics of non-crystalline solids. 1st ed. Amsterdam: North-Holland Publishing Co; 1965.
[42] Gaylord RJ, Weiss GH, DiMarzio EA. Macromolecules 1986;19:927–9.
[43] McKenna GB, Gaylord RJ. Polymer 1988;29:2027–32.
[44] Vallés EM, Macosko CW. Macromolecules 1979;12:673–9.
[45] Zang YH, Muller R, Froelich D. Polymer 1987;28-9:1577–82.
[46] Villar MA, Vallés EM. Macromolecules 1996;29:4081–9.
[47] Roth LE, Vallés EM, Villar MA. J Polym Sci Part A: Polym Chem 2003;41:1099–106.
[48] Macosko CW, Miller DR. Macromolecules 1976;9:199–206.
[49] Miller DR, Vallés EM, Macosko CW. Polym Eng Sci 1979;19:272–83.
[50] Miller DR, Sarmoria C. Polym Eng Sci 1998;38-4:535–57.
[51] Villar MA, Bibbó MA, Vallés EM. Macromolecules 1996;29:4072–80.
[52] Fetters LJ, Lohse DJ, Richter D, Witten TA, Zirkel A. Macromolecules 1994;27:4639–47.
[53] Urayama K, Yokoyama K, Kohjiya S. Macromolecules 2001;34:4513–8.